# GaN-based NDR Devices for THz Generation

**Egor Alekseev, Andreas Eisenbach, Dimitris Pavlidis,**
**Seth M. Hubbard and William Sutton**

Solid-State Electronics Laboratory
Department of Electrical Engineering and Computer Science
The University of Michigan, Ann Arbor, MI 48109-2122, USA

**Abstract**

GaN-based Negative Differential Resistance (NDR) diode oscillators have been studied by employing Gunn design criteria applicable to this material system. Numerical simulations were used to carry out large-signal analysis of the GaN NDR diode oscillators in order to evaluate their potential for THz signal generation. It was found that, due to the higher electron velocity and reduced time constants involved in the diode operation, GaN NDR diodes offer significantly higher frequency and power capability than conventional GaAs Gunn diodes. Based on the performed analysis, THz signal generation using GaN-based NDR diodes was predicted. GaN NDR layer structures were grown by MOCVD. The fabrication technology and characterization techniques used for GaN NDR diode oscillators are presented.

## I. Introduction

Active microwave diodes with negative differential resistance (NDR), such as GaAs or InP Gunn diodes, are the preferred devices for generation of microwave signals with high frequency and power. The frequency capabilities of Gunn diodes are limited by the rate of electron intervalley transfer. Thus, the amount of output power available from GaAs Gunn diodes decreases sharply when the oscillation frequency exceeds *100GHz*, which corresponds to the energy-relaxation time in this material of *~10ps* [1]. Due to larger threshold field in InP (*10.4KV/cm* vs. *3.5KV/cm* in GaAs), the energy-relaxation time in InP is shorter, and InP-based Gunn diodes with fundamental operation up to D-band frequencies have been demonstrated [2].

Studies of fundamental properties in III-V nitrides indicate that these wide-bandgap materials also exhibit bulk NDR effect with threshold fields in excess of *80KV/cm* [3,4,5]. Moreover, Monte Carlo studies of electron transport indicate that the energy-relaxation time in GaN is much shorter than in conventional III-V semiconductors [6,7]. Thus, use of GaN with increased electrical strength and reduced electron-transfer time constants offers the possibility to increase the frequency as well as the power-capability of NDR diode oscillators and extend the range covered by more traditional III-V semiconductor-based generators to THz frequencies.

In this work, large-signal numerical simulations are employed to investigate the suitability of GaN-based NDR diodes for millimeter and sub-millimeter (THz) signal generation. Based on the results of the large-signal simulations, several promising GaN NDR layer structures were selected and grown by MOCVD at the University of Michigan. Special device patterns and integrated circuits for experimental validation were developed. The fabrication technology and characterization techniques explored for realization and demonstration of GaN NDR diode oscillators are also discussed.

Work supported by ONR (Contract No. N00014-92-J-1552) and DARPA/ONR (Contract No. N00014-99-1-0513)

## II. Theoretical Basis for THz Signal Generation using GaN NDR Diodes

Studies of GaN-based NDR diodes were conducted by employing a commercial semiconductor-device simulator *Medici*. Since this program does not contain material parameters for GaN, these had to be obtained from literature and were evaluated, verified, and properly introduced into the simulator. Comparisons of simulated performance with experimental characteristics of GaN-based MESFETs and PIN diodes were made to enable validation of the selected parameters. Further details on the adopted approach are presented elsewhere [8].

A low-field electron mobility of $\mu_n=280cm^2/Vsec$ and $60cm^2/Vsec$ were assumed for wurtzite (*Wz)* GaN doped at $N=5\times10^{16}cm^{-3}$ and $1\times10^{19}cm^{-3}$, respectively [9]. The value of electron lifetime $\tau_n=7ns$ and hole lifetime $\tau_p=0.1ns$ used in the simulations was based on the experimental data measured by an electron-beam-induced current method [10]. Coefficients for calculating impact-ionization rates in GaN were obtained by fitting to the theoretical predictions presented in [11] and verified by comparing simulation results with experimental breakdown voltages reported for GaN PIN diodes [12].

Models for field dependence of electron mobility in GaN were based on the *v-F* characteristics calculated by Monte-Carlo simulations [13]. Velocity-field characteristics, evaluated in these studies, demonstrated a bulk NDR effect in the high-field region due to the intervalley transfer. However, the threshold field for intervalley transfer and consequent appearance of NDR in GaN was much larger than in conventional semiconductors such as GaAs. An increase of the threshold field is caused by a larger separation between the satellite and central valleys in *Wz* GaN where $\Delta E$ is $\approx 2.1eV$ compared to $\Delta E\approx 0.3eV$ for GaAs. The GaN *v-F* characteristic, used in the simulations, had a peak velocity $v_{PEAK}$ of $3\times10^7$, a saturation velocity $v_{SAT}$ of $2\times10^7$, and a threshold field $F_{TH}$ of $150KV/cm$.

According to recent studies of GaN bandstructure, the $\Gamma$-valley inflection point, at which the group electron velocity is maximal, was found to be located below the lowest satellite valley in both *Zb* (zinc-blende) [4] and *Wz* GaN [14]. Although further studies are necessary for experimental confirmation, the inflection point mechanism is also expected to cause bulk NDR in GaN. This contrasts other semiconductors, where intervalley transfer or impact ionization are initiated at a lower field than the inflection-point NDR [1].

The reported *v-F* characteristics of *Zb* GaN calculated using Monte Carlo simulations were based on a band structure containing the $\Gamma$-valley inflection point, and the results indicated that NDR was indeed caused primarily by the dispersion of the electron drift velocity in the $\Gamma$ valley [4]. The inflection-based NDR manifested a threshold field $F_{TH}$ of $80KV/cm$ and peak velocity $v_{PEAK}$ of $3.8\times10^7cm/sec$ compared with $F_{TH}=110KV/cm$ and $v_{PEAK}=2.7\times10^7cm/sec$ calculated in [3] for intervalley-transfer-based NDR. However, by far a more important consequence of the inflection-based NDR is the elimination of the intervalley-transfer relaxation time from the time required for NDR formation and, thus, a possibility of significantly increased frequency capability for GaN inflection-based NDR diodes.

Frequency-independent *v-F* characteristics can be used to describe electron transport in the presence of a time-varying electric field as long as the frequency of operation $f$ is much lower than the NDR relaxation frequency $f_{NDR}$ defined by $\tau_{ER}$ (the energy-relaxation time) and $\tau_{ET}$ (the intervalley relaxation time). The energy-relaxation time of $0.15ps$ calculated for *Wz* GaN was ten times smaller than the GaAs value of $1.5ps$. The intervalley-transfer relaxation time $\tau_{ET}$ was

evaluated from the results of Monte Carlo studies of ballistic transport [15]. By extrapolating reconstructed $\tau_{ET}(F)$ curves to the point of threshold field $F=F_{TH}$, electron intervalley transfer times $\tau_{ET}$ of *7.7ps* and *1.2ps* were found for GaAs and GaN, respectively.

Based on the results of this estimation, the NDR relaxation frequency $f_{NDR}$ of GaAs was found to be *~100GHz* in excellent agreement with experimental and theoretical results [1]. The frequency capability of GaN-based NDR devices was found superior to that of GaAs Gunn diodes as indicated by the GaN NDR relaxation frequency $f_{NDR}$ of *~1THz* for the case of intervalley-transfer-based NDR and *~4THz* for case of inflection-based NDR (with $\tau_{ET}=0ps$). Since the equation and the frequency-response of *v-F* characteristics in GaN is not yet well-determined, both intervalley-transfer-based NDR of *Wz* GaN and inflection-based NDR of *Zb* GaN were considered in order to account for uncertainty in published *v-F* characteristics.

Overall, GaN offers higher peak and saturation velocities than GaAs, which leads to reduced transit time and increased frequency of operation. The threshold and breakdown fields are also larger in GaN, which allows operation at a higher bias and leads to increased output power. The increased frequency response of high-energy electrons in GaN is attributed directly to the higher electrical strength of this material compared with GaAs. The THz capability, predicted for GaN devices operating on the inflection-based NDR, is possible due to the exceptionally high frequency response of electrons to the variations of the bandstructure as suggested in [4].

## III. Design of GaN-based NDR Diodes for THz Sources

When a high electric field $F > F_{TH}$ is applied to bulk GaN, electrons experience a negative differential mobility $\mu_{NDR}$. Under these conditions, a non-uniformity of electron concentration would grow at a rate $1/\tau_{DD}$, where $\tau_{DDR}$ is the differential dielectric relaxation time and depends on the electron concentration $N$, the dielectric constant $\varepsilon$, and the peak negative differential mobility $\mu_{NDR}$. It is recognized that domain growth lasts for at least $3\times\tau_{DDR}$ [16] and, thus, the operation frequency of NDR devices can be limited by the active layer doping. The dependence of frequency capabilities on $N$ for GaN and GaAs was calculated using their respective material parameters and the results are presented in Figure 1.

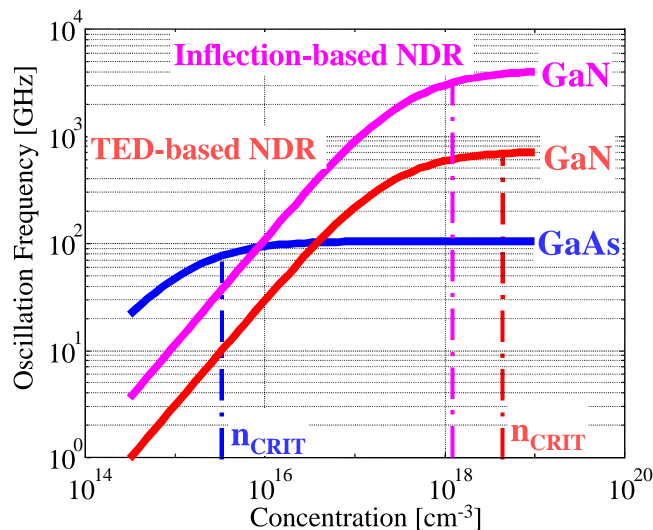


Figure 1. Concentration-frequency diagram of Gunn diodes made of GaAs and GaN

The negative differential mobility in GaAs is larger than in GaN and, therefore, for low doped devices, growth of electron domains occurs faster in GaAs than in GaN. However, as $N$ is increased, $\tau_{DDR}$ is reduced, and the frequency capability improves until it reaches the NDR relaxation frequency $f_{NDR}$ discussed in the previous section. Since $f_{NDR}^{GaAs} < f_{NDR}^{GaN}$ the frequency capability of GaN-based devices improves for higher $N$ without being limited by $f_{NDR}$ as in case of GaAs. This leads to GaN NDR operation that exceeds the GaAs limit of $105GHz$ for GaN doping levels above $5\times10^{16}cm^{-3}$.

($N\times L$) criteria for the possibility of Gunn domain instability are based on the fact that the domain growth rate $1/\tau_{DDR}$ should be higher than the transit frequency $f_T = v_{PEAK}/L_A$:

$$(N_A \times L_A) > (N \times L)_0 \equiv \frac{3\times\varepsilon\times v_{PEAK}}{q\times\mu_{NDR}} \qquad (1)$$

where $N_A$ is the doping, $L_A$ is the thickness of the active layer, $(N\times L)_0$ is the critical value of the ($N\times L$) product, and the factor $3$ accounts for the domain growth time, as explained earlier. The critical values of ($N\times L$) product for GaN and GaAs were calculated using (1), and the results showed that, due to a higher peak velocity and a smaller negative mobility, $(N\times L)_0$ for GaN is $\sim10^{13}cm^{-2}$ which is an order of magnitude larger than for GaAs ($10^{11}$-$10^{12}cm^{-2}$).

However, if the active layer doping ($N_A$) exceeds the critical doping concentration $N_{CRIT}$, static domains can be formed inside the active layer [16]. Formation of parasitic static domains results in a decrease of output power and may lead to an early breakdown. Due to the large difference in threshold electric fields ($F_{TH}$), $N_{CRIT}$ in GaN calculated according to (2) [16]

$$N_{CRIT} = \frac{\varepsilon\times F_{TH}^{\ 2}}{q} \qquad (2)$$

is much higher than in GaAs and, thus, the active region in GaN diodes can be doped significantly higher ($\sim10^{17}cm^{-3}$) than in GaAs designs ($\sim10^{15}cm^{-3}$). The latter is a very important since the availability of low-doped GaN material ($N_A < 5\times10^{16}cm^{-3}$) is limited. Higher doping of active layers in GaN NDR diodes also leads to reduction of $\tau_{DDR}$ in this material, helping to increase its frequency capability. Due to the higher doping of the active layer in GaN NDR diodes, the devices are operated at a higher current level which leads to an increased level of output power.

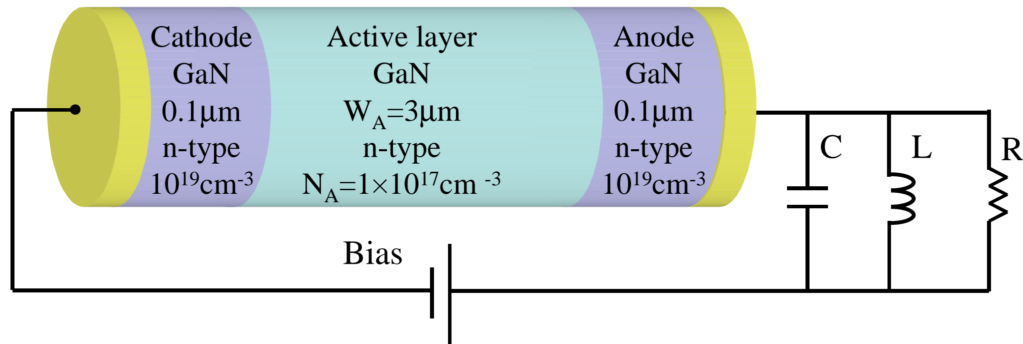


Figure 2. Schematic of GaN NDR diode oscillator.

A typical GaN NDR diode designed to operate at ~*100GHz* had an n-type active layer with thickness $L_A$ of $3\mu m$ and doping $N_A$ of $1\times10^{17}$ cm$^{-3}$. The active layer was sandwiched between anode and cathode layers and their corresponding ohmic contacts. Both contact layers were $0.1\mu m$-thick and doped at $1\times10^{19} cm^{-3}$. The diameter of the diode $D$ was selected to be $50\mu m$. A final three-dimensional model of GaN NDR diode oscillator is shown in Figure 2 together with the bias supply and a parallel *LCR* circuit used to represent the resonant cavity.

## IV. Operation of GaN-based NDR Diode Oscillators

Custom *hydrodynamic* simulators have previously been used for studies of Gunn diodes [17,18]. The commercial simulator employed in our work also offers hydrodynamic capabilities, and has been used for large-signal power characterization of GaN NDR diode oscillators and, for comparison purposes, with GaAs Gunn diode oscillators. The equations used in the hydrodynamic simulations of GaN NDR diodes included Poisson's equation, carrier-continuity equations, and electron energy-balance equations. By including the NDR relaxation time $\tau_{NDR}$ in the energy relaxation time used in the energy-balance equations, NDR in *v-F* characteristics was constrained to frequencies lower than the NDR relaxation frequency $f_{NDR}$.

When a bias $V_D$ exceeding the critical value $V_{CR}=F_{TH}\times L_A$ is applied to the anode contact it results in an electric field $F>F_{TH}$. Under such conditions, the GaN NDR diode may become unstable and produce sustained oscillations. The power and frequency of the oscillations depend on the device design, biasing conditions, and termination impedance of the resonant cavity $Z_L$. The effect of the latter was modeled by adding a parallel *LCR* circuit as shown in Figure 2.

Thus, a $W_Z$ GaN NDR diode designed for W-band operation was biased using $V_D=2\times V_{CR}=90V$ and connected to the *LCR* circuit with $L=17.5pH$, $C=0.1pF$, and $R=50\Omega$. Starting at time zero, $V_D$ was increased from *0* to *90V* with a large rise time of *>1ns* in order to minimize voltage overshoot. The growth of oscillations takes place over *0.5ns,* and is followed by a region of sustained oscillations. The dynamic *I-V* trace corresponding to sustained oscillations is shown in Figure 3 together with a stable DC I-V curve simulated for case when the GaN diode was connected directly to a voltage source.

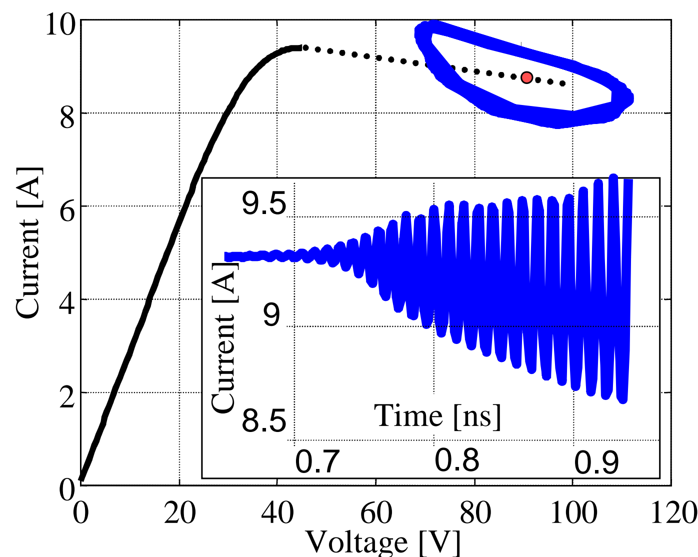


Figure 3. *I-V* trace of observed oscillations (build-up of oscillations is shown on the inset).

The figure also shows gradual build-up of the amplitude of current oscillations. Finally, voltage and current waveforms in the region of sustained oscillations were subjected to harmonic power analysis based on Fourier transformed and the obtained spectrum was used to determine the output power and the oscillation frequency.

The power and frequency capability of GaN NDR diodes were compared with that of GaAs Gunn diodes by simulating the performance of the corresponding oscillators. The nominal GaAs Gunn diode had the same dimensions as the nominal GaN NDR diode: $L_A=3\mu m$ and $D=50\mu m$, but the doping was reduced to $3\times10^{15}$cm$^{-3}$ in order to satisfy the design condition $N_A < N_{CRIT}$ (see previous section). This design of GaAs Gunn diode was analogous to published descriptions of Ka-band Gunn diodes in reference [19]. The bias $V_D$ for both GaN- and GaAs-based devices was selected to be twice the critical bias $V_{CR}$ and, for nominal designs, was *90V* and *2.1V*, respectively. Designs of *LCR* circuits were optimized to provide maximum output power when used with devices of nominal designs. The results obtained for GaAs and GaN diodes with varying thickness of the active layer are shown in Figure 4.

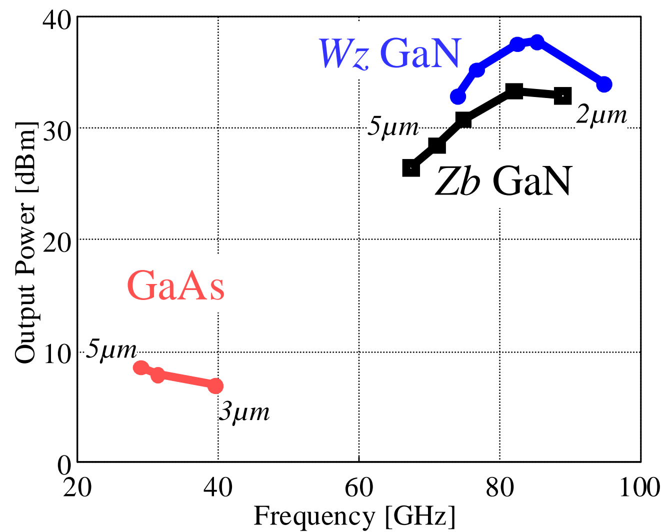


Figure 4. Frequency-power diagram comparing GaAs and GaN NDR diodes

The simulations were conducted for the NDR diodes made of both *Wz* and *Zb* phases of GaN in order to account for uncertainty in published *v-F* characteristics. The simulations showed that the overall characteristics of GaN-based NDR diodes outperform those of GaAs Gunn diodes in terms of output power and frequency of oscillations independent of the specific *v-F* characteristics used to model material properties of GaN. Thus, given the same thickness of the active layer, the operation frequency of GaN NDR diodes (*65-95GHz*) was approximately twice that of GaAs Gunn diodes (*27-40GHz*), while given the same device area, the maximum output power of GaN NDR diodes was *~35dBm* compared with *~10dBm* for GaAs Gunn diodes.

The possibility of fundamental THz signal generation using GaN-based sources was investigated by optimizing the design of GaN NDR diodes for operation at higher frequency. Thus, following the results of Figure 1, the thickness of the active layer was reduced from *3* to $0.3\mu m$ in order to reduce transit time while the doping of the active layer was increased from $10^{17}cm^{-3}$ to $10^{18}cm^{-3}$ in order to reduce the dielectric relaxation time. At the same time, the size of the diode was decreased from *50* to $10\mu m$, which allowed minimization of parasitic shunt capacitance as required for operation at submillimeter-wave frequencies. Large-signal

hydrodynamic simulations of the THz GaN NDR diode with $0.3\mu m$-thick $10^{18} cm^{-3}$-doped active layer revealed appearance of sustained oscillations with fundamental frequency exceeding *700GHz* as illustrated by the output power spectra in Figure 5.

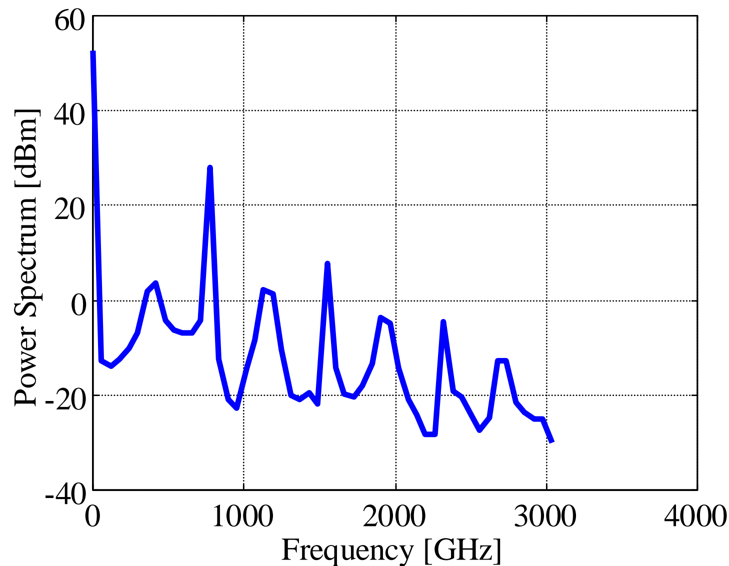

Figure 5. Simulated output power spectrum of THz GaN-based NDR oscillator.

## V. MOVPE Growth of GaN NDR Diode Layers

Layers have been grown by metalorganic vapor-phase epitaxy (MOVPE) in a home-built horizontal quartz reactor. Substrates were placed on a graphite susceptor, which is heated by *10KW* RF generator. Growth was performed at low pressure (*60 – 110torr*) on c-plane sapphire substrates using *TMGa*, *TMAl*, and $NH_3$ as precursors. First, a thin, *~20nm* thick GaN buffer layer was grown at *515℃*, followed by the high-temperature growth of the bulk GaN layers at *1120℃*. Growth rates for GaN were $\sim 1.4\mu m/h$ using a V/III ratio of *~1600*.

Using the low-temperature GaN-buffer approach, high-temperature grown undoped bulk GaN layers were smooth, transparent, and uniform. GaN layers with low background carrier concentration are required for successful development of NDR diodes. In addition, NDR diodes use contact layers, which should be highly n-doped to allow for low contact and access resistances. GaN growth conditions for the bulk and especially for the buffer layer have been carefully optimized to satisfy those requirements. After optimization of the buffer thickness, increasing the reactor pressure from *60* to *110torr* during both buffer and bulk GaN growth led to a decrease of the background carrier concentration by *50%* to less than $2{\times}10^{17} cm^{-3}$ in thin ($\sim 0.7\mu m$) GaN test layers. Further increase of the reactor pressure led, however, to a deterioration of the electrical characteristics. Increasing the layer thickness to only $1.4\mu m$ further decreased the background carrier concentration by another *50%* to $1.2{\times}10^{17} cm^{-3}$, while at the same time increasing the mobility by *20%*, thus providing good material quality for NDR device applications.

Si-doped GaN layers have been grown and investigated to provide low-resistance contact layers for the NDR diodes. Carrier concentration has been found to depend linearly on the $Si_2H_6$ source flow. While Hall mobility decreases with increasing carrier concentration, high-doped contact layers ($n=1{\times}10^{19} cm^{-3}$) still have $\mu > 100cm^2/Vsec$.

After completing the test layers and growth parameter optimization, NDR diode device structures have been grown. The cross-section of the GaN NDR diodes consisted (starting from the top) of the anode layer ($n^+=1\times10^{19}cm^{-3}$, $t=0.15\mu m$), the active layer ($n^-=1\text{-}2\times10^{17}cm^{-3}$, $t=2.5\mu m$), and the cathode layer ($n^+=1\times10^{19}cm^{-3}$, $t=0.5\mu m$).

## VI. Fabrication and Characterization of GaN NDR diodes

The NDR diodes were realized on circular mesas formed by dry etching. First, isolation mesas were formed by removing all GaN layers outside the active device area down to the sapphire substrate. Secondly, anode mesas were formed by etching through the anode and active layers down to the second n+ (cathode) layer. For the experimental layers investigated here, this required *4.6μm*-deep isolation etch and *3.1μm*-deep anode mesa etch. The dry etching was performed in a low-pressure RIE (*15mT*) in $CCl_2F_2:Ar_2$ (*1:1*) atmosphere. The RF power for plasma generation was set to *150W*. This technology employs Ti/Ni masks and produces mesas with near-vertical walls with a GaN etch rate of *50nm/min*. GaN-based NDR diodes employ two ohmic contacts: anode and cathode. The anode contact was deposited on the top $n^+$ layer and the cathode was deposited on the bottom $n^+$ layer. *Ti/Al/Ti/Au/Pt* metals were used for cathode ohmic contacts. *Ti/Ni* metals used for etching mask were used to realize the anode contact on the top n+ layer. Ohmic metallization was followed by plating of Au interconnects, airbridges, and probing pads combined with integrated on-wafer heatsinks. A fabricated GaN NDR diode suitable for high-frequency on-wafer testing is shown in the SEM photograph of Figure 6.

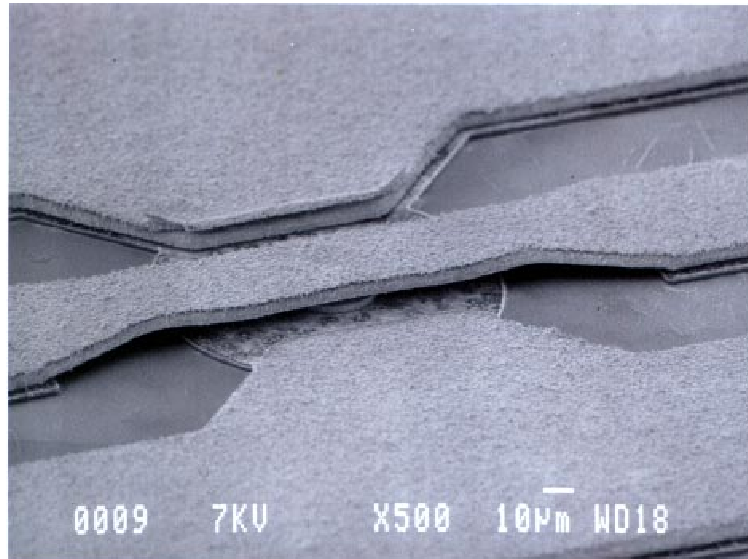


Figure 6. SEM photograph of fabricated GaN NDR diode

Electrical characterization of the fabricated devices revealed increased voltage and current capabilities of the GaN-based NDR diodes. Thus, pulsed I-V characteristics for biasing voltage $V_D$ and current $I_D$ up to *40V* and *1A*, respectively, were recorded. However, the low thermal conductivity of sapphire substrates (*0.3W/Kcm*) led to self-heating of the integrated devices and prohibited application of DC or pulsed biases required for further testing. Use of GaN NDR diode layers grown on SiC substrates with high thermal conductivity (5W/Kcm) or removal of sapphire substrates by laser-ablation is planned to be employed in future fabrication runs to improve the efficiency of heat removal.

## VII. Conclusions

The microwave characteristics of GaN NDR diode and GaAs Gunn diode oscillators were evaluated by performing large-signal harmonic power analysis of current and voltage waveforms corresponding to sustained oscillations. The analysis showed that GaN-based NDR diodes outperform GaAs Gunn diodes independent of the specific *v-F* characteristics used to model material properties of GaN. GaN NDR diodes optimized for THz operation demonstrated a possibility of fundamental operation with frequency exceeding *700GHz*. The increased frequency capability offered by GaN NDR sources is due to a significantly higher electrical strength of this wide-bandgap material which allows operation with thinner and higher-doped active layers, compared to that of Gunn diodes made of conventional III-V compounds. GaN NDR layers designed for W-band operation were grown on sapphire substrates and integrated GaN NDR diodes were fabricated using dry etching techniques. Electrical characterization of the fabricated devices revealed their high voltage and current capabilities. Laser ablation techniques are expected to allow fabrication of devices with low thermal resistance as required for device optimization.

## References


[1] P. J. Bulman, G. S. Hobson, B. C. Taylor, "Transferred Electron Devices", Academic Press, London and New York, 1972

[2] H. Eisele and G. I. Haddad, "Efficient power combining with D-band (110-170GHz) InP Gunn devices in fundamental-mode operation", *IEEE Microwave and Guided Wave Letter*, vol.8, no.1; Jan. 1998; p.24-6

[3] J. Kolnik et al., "Electronic Transport Studies of bulk zinc-blende and wurtzite phases of GaN based on an ensemble Monte Carlo calculation including a full zone bandstructure", *J. Appl Phys*, 78 (2), July 1995, p 1033-1038

[4] S. Krishnamurthy et al, "Bandstructure effect on high-field transport in GaN and GaAlN", *Applied Physics Letters*, 71 (14), 6 October 1997, p 1999-2000

[5] E. Alekseev and D. Pavlidis, "Microwave Potential of GaN-based Gunn Devices", *Electronics Letters*, vol. 36, no. 2, 20 January 2000, p. 176-178

[6] B. E. Foutz et al., "Comparison of high field electron transport in GaN and GaAs", *Appl Phys Lett*. 70 (21), 1997, p 2849-2852

[7] S. Wu, A. F. M. Anwar, "Monte-Carlo Simulation in Submicron GaN $n^+nn^+$ Diodes", *1999 International Semiconductor Device Research Symposium*, Charlotesville, VA, Dec. 1-3, 1999

[8] E. Alekseev and D. Pavlidis, "DC and High-Frequency Performance of AlGaN/GaN Heterojunction Bipolar Transistors", *Solid-State Electronics,* , v. 44, n. 4, p 245-252, April 2000

[9] S. N. Mohammad and H. Morcoç, "Progress and Prospects of Group-III Nitride Semiconductors", *Prog. Quant. Electr*., vol.20 no 5/6, pp. 361-525, 1996

[10] Z. Z. Bandic et al., "Nitride Based High Power Devices: Transport Properties, Linear Defects, and Goals", *1998 MRS Symposium Proceedings*, Vol. 512, p 27-32, 1998

[11] J. Kolnik et al., "Monte Carlo calculation of electron initiated impact ionization in bulk zinc blende and wurtzite GaN", *J. of Appl. Phys.*, vol. 81 (12), p 727-733, 1997

[12] V. A. Dmitriev et al., "Electric Breakdown in Nitride PN Junctions", *MRS Symposium Proceedings*, vol. 395, p 909-912, 1996

[13] U. D. Bhapkar and M. S. Shur, "Monte Carlo calculation of velocity-field characteristics of wurtzite GaN", *J. Applied Physics*, 82(4), p 1649-1655, 1997

[14] A. B. Chen (see also [4]): private communications

[15] B. E. Foutz et al., "Comparison of high field electron transport in GaN and GaAs", *Appl. Phys. Lett*. 70 (21), p 2849-2852, 1997

[16] M. Shur, "GaAs Devices and Circuits", Plenum Press, New York and London, 1987

[17] M. F. Zybura et al., “100-300 GHz Gunn oscillator simulation through harmonic balance circuit analysis linked to a hydrodynamic device simulator”, *IEEE Microwave and Guided Wave Letters*, V. 4, N. 8, p 282-284, 1994

[18] V. A. Posse and B. Jalili, "Gunn effect in heterojunction bipolar transistors", *Electronics Letters*, Vol. 30, No. 14, p. 1183-1184, 1994

[19] T. G. Ruttan, “High-Frequency Gunn Oscillators”, *IEEE Transactions on Microwave Theory and Techniques*, p 142-144, February 1974